



Journal of Ultrafine Grained and Nanostructured Materials

<https://jufgnsm.ut.ac.ir>

Vol. 53, No.2, December 2020, pp. 166-176

Print ISSN: 2423-6845 Online ISSN: 2423-6837

DOI: [10.22059/jufgnsm.2020.02.08](https://doi.org/10.22059/jufgnsm.2020.02.08)

The surface modification of Nitinol superelastic alloy with alkaline-heat treatment and hydroxyapatite/chitosan composite coating for biomedical applications

Leila Fathyunes*, Seyed Omid Reza Sheykholeslami

*Department of Materials Science and Engineering, University of Bonab, Bonab, Iran.
Research Center for Advanced Materials, Faculty of Materials Engineering, Sahand University of Technology, Tabriz, Iran.*

Received: 29 September 2020; Accepted: 28 October 2020

** Corresponding author email: fathyunes.leila@gmail.com*

ABSTRACT

In the present work, the surface modification of Nitinol was carried out by a two-step process consisting of pretreatment and applying the bioactive composite coating to extend its biomedical applications. For pretreatment, we used a combination of chemical etching, boiling in distilled water and alkaline-heat treatment. According to the results of Raman and grazing-incidence X-ray analysis, the surface layer formed on the pretreated Nitinol was consisted of rutile phase and sodium titanate phases. The pretreatment significantly decreased the concentration of Ni ions released from Nitinol alloy into Ringer's solution during 10 days immersion from 126.6 ppb to 5.3 ppb. Moreover, this pretreatment process did not have the negative effect on the superelasticity of the Nitinol alloy. In the following, we used a composite coating of hydroxyapatite/chitosan on the pretreated Nitinol. This coating was applied using one-step cathodic electrophoretic deposition from suspension containing 5 g/L hydroxyapatite and 0.5 g/L chitosan at different voltages of 30, 40 and 50 V/cm². A uniform coating with acceptable quality was obtained by electrophoretic deposition at 40 V/cm² for 120 s. The morphology of this coating was studied using scanning electron microscope and Fourier transform infrared spectroscopy analysis. The findings confirmed fabrication of a crack free morphology, which was consisted of hydroxyapatite and chitosan. Finally, according to the results of potentiodynamic polarization test, the corrosion current density for bare, pretreated and pretreated/coated Nitinol were calculated about 2.63, 1.94 and 0.75 $\mu\text{A}/\text{cm}^2$, indicating the effect of pretreatment and applying hydroxyapatite/chitosan coating on decreasing the corrosion rate of Nitinol.

Keywords: Nitinol, Pretreatment, Hydroxyapatite, Chitosan, Electrophoretic deposition, Ni ions release.

1. Introduction

Nickel-titanium (Nitinol) superelastic alloy as an intermetallic compound is one of the most promising biomaterials in today's world due to its unique physical and mechanical properties like super-elasticity, shape memory effect, relatively low elastic modulus and good biocompatibility

[1, 2]. Nitinol alloy has the elastic modulus in the range of 55-80 GPa, which is close to the modulus of bone (about 30 GPa) as compared to the other metals used in the manufacturing of permanent implants like Ti alloys (110 GPa) and 316 L stainless steel (200 GPa). Moreover, the recoverable strain up to 10% is reported for

Nitinol, whereas the recoverable strain of human bone and 316 L stainless steel are only 2% and 0.5%, respectively. The mentioned mechanical properties cause a proper distribution of stress at the interface of Nitinol implant/surrounding tissues and therefore acceleration of bone growth [3]. However, the high Ni content of this alloy (nearly 50 at.%) leads to the releasing of a significant amount of toxic Ni ions with time after its implantation in the human body mainly owing to corrosion in the physiological environments [4-6]. Elimination of the surface nickel and preparation of a barrier layer like titanium oxide on its surface are desirable solutions to reduce the Ni ions release during long-term implantation [7]. On the other hand, the bioactivity of implant as well as the biomechanical integrity at the bone/ implant interface are very vital in biomedical applications. Nevertheless, Nitinol alloy has the bio-inert nature and shows poor osteoinductive properties when is implanted in a human body. Therefore, it is necessary to improve the surface bioactivity of this alloy [1, 8]. In the recent decades, various surface treatment methods such as acid-etching, heat treatment, anodizing and applying bioactive coatings such as hydroxyapatite (HA) have been developed for this purpose [8-10].

HA with chemical formula of $\text{Ca}_{10}(\text{PO}_4)_6(\text{OH})_2$ has been widely used as a biocompatible and bioactive ceramic in medical applications due to its structural and chemical similarity to the main mineral component of human hard tissues [9-13]. In fact, the surface functionalization of metallic implants with applying the HA coating leads to achieve a combination of the good mechanical properties of metal substrate and bioactivity of this coating [14]. Among several coating methods, electrophoretic deposition (EPD) is a simple and flexible technique with low cost of equipment, which enables a good control over the thickness, morphology, crystallinity, and stoichiometry of the coatings [1, 13]. The coating deposited using this method commonly requires sintering at relatively high temperatures to provide sufficient adhesion to the substrate. However, sintering brings some challenges such as oxidation of substrate, degradation and shrinkage of the HA coating, and generation of the significant internal stresses within the coating due to difference in the thermal expansion coefficients of the coating and the substrate [13, 15, 16]. Fortunately, these problems could be effectively solved via applying the polymer-ceramic composite coatings, as the

sintering is not required for these type coatings [9, 16]. Chitosan (CS) as a derivative of chitin is a natural cationic polymer, which has a structural similarity to glucosamine of the bone extracellular matrix and therefore is a good candidate for tissue engineering applications [13, 17]. Because of having the excellent properties including non-toxicity, biocompatibility, biodegradability and antibacterial property [18], the incorporation of this polymer into the HA coating not only improves the adhesion of this composite coating to substrate without any sintering [9, 19, 20], but also provides more biocompatibility [9]. Moreover, the natural bone is a nanocomposite material with the organic-inorganic laminate structure containing about 70 wt. % of HA, so applying the HA/CS composite coating on the metallic implants could be useful to mimic the structure and properties of the natural bone on the surface of these implants [15, 21]. The favorable bioactivity of the HA coating could also provide a suitable condition in body for the adhesion of bacteria on the implant surface resulting in the infection and failure of implantation. In this regard, CS with antibacterial activity acts as an effective composite component to reduce the postoperative infections [20, 22, 23].

With these in mind, the objective of the present paper is the surface modification of the Nitinol alloy to make it more appropriate for biomedical applications. For this purpose, we developed a homogeneous coating via co-deposition of HA and CS by EPD method on Nitinol alloy. The HA used in this study was extracted from bovine cortical bone, which has more chemical and structural similarity to the bone and therefore it seems to be an alternative for synthetic HA [1]. Before applying the HA/CS composite coating, the pretreatment of Nitinol alloy was carried out by a combination of acid-etching and alkaline-heat treatment to reduce the Ni ions release from this alloy into the physiological environments. The morphology, chemical and phase composition of the surface layer formed on the pretreated Nitinol and the HA/CS coating were investigated. Furthermore, the effect of pretreatment and applying the HA/CS composite coating on the corrosion stability of Nitinol in Ringer's solution was also examined using potentiodynamic polarization test.

2. Materials and methods

2.1. Pretreatment of Nitinol

In this work, a combination of chemical etching,

boiling in distilled water and alkaline-heat treatment processes was used to pretreat the surface of Nitinol alloy before applying the composite coating. Firstly, Nitinol rod with nominal composition of 50.9 at. Ni and diameter of 12.6 mm were cut into thickness of 1 mm. The surface of these samples was grinded up to 1200 mesh followed by cleaning successively in acetone and ethanol in an ultrasonic bath for 15 min and finally they were rinsed with distilled water. Then, the samples were chemically etched in the solution of $1\text{HF} - 4\text{NHO}_3 - 5\text{H}_2\text{O}$ at least for 4 min and soaked in boiling water for 20 min. In fact, this stage was carried out to eliminate the defects and scratches of the surface as well as to leach nickel of the surface [7, 8]. For alkaline-heat treatment, the etched samples were soaked in 5M NaOH aqueous solution at 60 °C for a period of 24 h followed by rinsing with distilled water [24-26]. In this stage, sodium and oxygen ions could penetrate into the surface of Nitinol alloy. At last, heat treatment of these samples was carried out under low oxygen pressure atmosphere [7, 27]. For this purpose, the alkaline treated samples were encapsulated in a glass tube purged for several times with argon gas [8]. Moreover, titanium foils, which are susceptible to oxidation reactions, were placed inside this tube for further purification of the atmosphere from oxygen. Eventually, the samples were heat treated at 500 °C for 30 min [8].

2.2. Synthesis of HA Powder

As mentioned before, about 70% by weight of adult bone consists of HA. Hence, in the present work we used the natural source of bone for extraction of HA powder, because it is cheaper than the synthetic HA. For this purpose, the bovine cortical bone was burned by flame in air. Then, the obtained black powder was heat treated in an air atmosphere furnace at 800 °C for 2 h. In this stage, this black powder converts to a white crystalline HA powder. Finally, the milling operation of powder was performed in a ball mill for 2 h [1].

2.3. Applying the HA/CS composite coating on the pretreated Nitinol alloy

The HA/CS composite coatings were applied by EPD technique from suspension of 5g/L HA in a mixed ethanol-water solvent (17 vol.% water) which is containing 0.5g/L CS and 1 vol.% acetic acid. The water and acetic acid were used for dissolution of CS. According to the previous study reported by Mahmoodi et al., the more water content degrades

the quality of this coating because of a considerable evolution of hydrogen gas at cathode during the EPD process [13]. Medium molecular weight CS purchased from Sigma Aldrich with a degree of deacetylation of 75-85% was used to prepare this suspension. Firstly, the CS powder was dissolved into the 1 vol.% acetic acid (99.8%, Merck) solution at room temperature with magnetic stirring and HA was ultrasonically dispersed in ethanol. After that, the CS solution was added to the HA suspension. Before EPD, this suspension was sonicated for 10 min to achieve a homogeneous dispersion. An electrophoresis cell was designed with a 100 mL beaker in which pretreated Nitinol as a cathode and graphite as anode were fixed with constant distance about 1 cm. The EPD process was done for 120 s at a constant voltage of 30, 40 and 50 V/cm² applied by a DC power supply and the change of weight and current density were recorded. At last, the coated samples were dried in desiccator at room temperature for 24 h.

2.4. Characterization

The phase analysis of the thin film formed on the pretreated sample was performed by XRD device (PANalytical-X'Pert Pro MPD-Netherlands) in grazing-incidence beam (GIB) mode with Cu K_a radiation generated at 40 kV, 40 mA, and the incident beam angle of 1°, with a step size of 0.026 deg, and a step time of 48 seconds.

A Raman spectrum for the pretreated Nitinol was measured using a SENTERRA-BRUKER spectrometer and an incident wavelength of 532 nm from an argon ion laser over a range of 200–700 cm⁻¹.

The surface morphology of the pretreated and coated samples were studied using scanning electron Microscope (SEM, Cam Scan MV2300, Vega Tescan, Czech Republic) coupled with energy dispersive spectroscopy (EDS) and field emission scanning electron microscope (FE-SEM, Tescan MIRA3 FEG-SEM, Czech republic). For this purpose, the samples were covered with a very thin layer of gold using sputter coater for avoiding electrical charging.

In order to determine the effect of pretreatment on the Ni ions release from Nitinol alloy, the grinded and pretreated samples were immersed in 30 mL of the Ringer's solution at the temperature of 37 °C for 10 days. After that, the concentration of the Ni ions released into this solution was detected by a graphite furnace atomic absorption

spectroscopy (PerkinElmer, Germany).

To evaluate the superelastic behavior, the stress-strain curves of the as-received and pretreated samples were obtained using a Santam (STM50) tensile testing device equipped with an electrical oven at a cross-head speed of 2 mm/min and temperature of 37 °C in a loading and unloading course up to 5.5% strain.

The chemical bands of the chitosan powder and the HA/CS coating were studied by Fourier transform infrared spectroscope (FTIR, Bruker Tensor 27, Germany). For this purpose, each of the purchased CS and the HA/CS coating scrapped from the surface separately mixed with about 80% KBr in weight and were pressed into transparent discs. Then, their analysis was done in transmittance mode at wavenumber ranging from 400 to 4000 cm⁻¹.

The potentiodynamic polarization test was conducted by Potentiostat/Galvanostat Autolab (model PGSTAT302N) at a constant scan rate of 0.1 V/s to investigate the corrosion behavior of bare Nitinol as well as pretreated and coated samples in Ringer's solution at 37 °C. For this test, saturated calomel electrode (SCE) and platinized platinum electrode were used as the reference and auxiliary electrodes, respectively. Before the polarization test, the samples were immersed in the Ringer's solution for 30 minutes to reach a stable condition.

3. Results and discussion

3.1. Characterization of the pretreated Nitinol

Fig. 1 shows optical images of the solution used for etching and the surface states of Nitinol before and after chemical etching. The etched surface becomes rough and cloudy and the color of etching solution changes to green, which is due to the leaching of Ni ions from the surface and therefore the presence of these ions in this solution. In fact, chemical etching is beneficial for removing the impurities and Ni ions from the surface of Nitinol alloy. Moreover, boiling the etched samples in

distilled water provides the better condition for Ni ions release by promoting the diffusion of Ni atoms to the interface of Nitinol surface and water. It was reported that with this method the Ni ions is depleted in a depth of 5-10 nm from surface [7].

Fig. 2 shows GIB pattern of the pretreated Nitinol alloy. Besides the Bragg peaks related to Nitinol substrate (ICDD: 00-018-0899) and Ni₄Ti₃ precipitates (ICDD: 00-039-1113), some other peaks are appeared in this pattern relating to the formation of oxide layer on the pretreated sample. These peaks reveal that the formed surface layer is consisted of sodium titanate (ICDD: 00-013-0589) and rutile (ICDD: 00-003-1122) phases. As mentioned before, a surface depletion from nickel as well as the high chemical affinity of titanium to oxygen could result in the oxidation of titanium rather than nickel.

A typical Raman spectrum of the pretreated Nitinol is also reported in Fig. 3. The characteristic rutile modes of E_g (447cm⁻¹) and A_{1g} (612 cm⁻¹) comes from the passive layer formed on the pretreated sample [30]. Moreover, the asymmetric shape of the band appeared between 211-261 cm⁻¹ suggest the overlapped second order Raman scattering band of rutile (237 cm⁻¹) and the sodium titanate band (around 274 cm⁻¹) [30, 31].

Fig. 4 shows FE-SEM images and EDS point-analysis spectrum obtained from the pretreated surface of Nitinol alloy. After pretreatment process, a warm-like nanostructure layer with fine pores is formed on the surface, as is observed from Figs. 4 a and b. This porous layer could improves the adhesion of the next HA/CS layer to the Nitinol surface with changing the surface roughness. The EDS analysis of the pretreated sample in Fig. 4 c reveals the presence of not only Ni and Ti, but also Na and O elements. These elements could be attributed to the presence of sodium titanate and rutile phases in the surface layer of the pretreated sample, as previously shown by the results of GIB and Raman analysis. In fact, the formation of

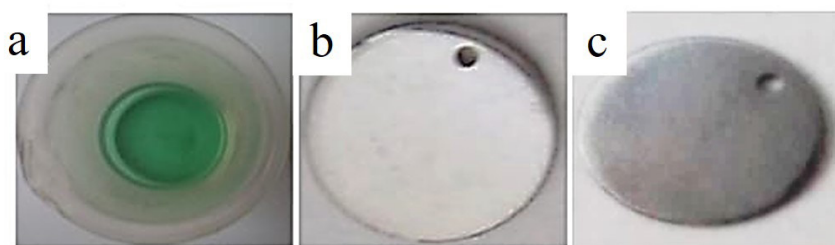


Fig. 1- Optical images of a) the solution used for etching and Nitinol samples b) before and c) after chemical etching.

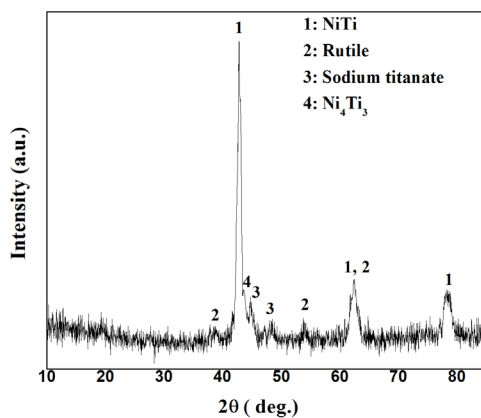


Fig. 2- The GIB pattern of the pretreated Nitinol alloy.

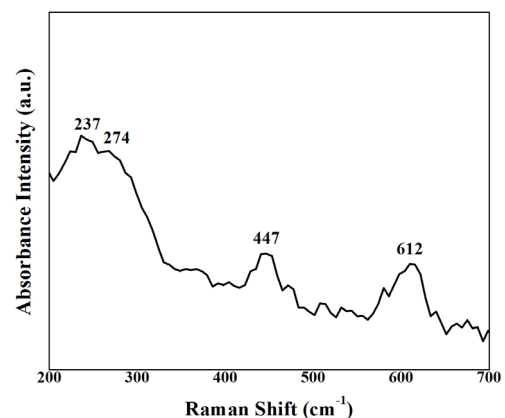


Fig. 3- Raman spectrum of the pretreated Nitionl alloy.

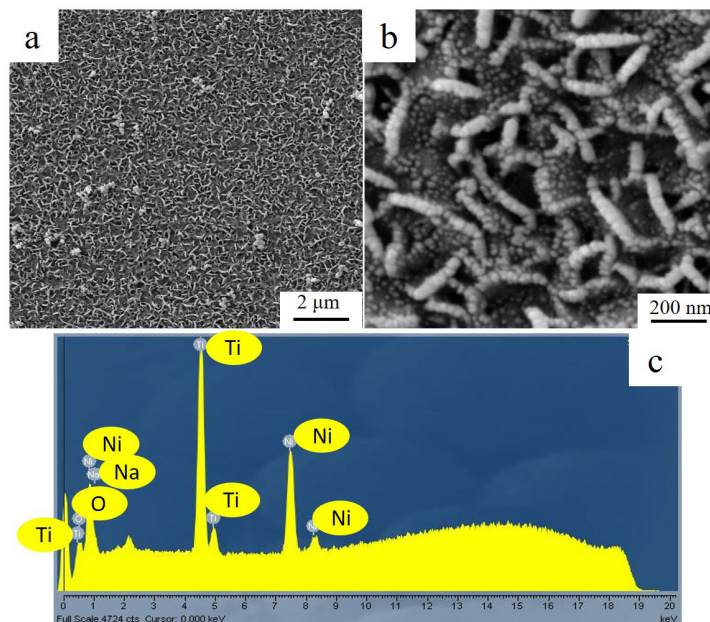


Fig. 4- FE-SEM images taken from the surface of pretreated Nitinol at magnification of a) 10000 x, b) 100000 x and c) EDS spectrum obtained from point-analysis on this surface.

rutile phase (TiO_2) could be due to the difference in oxidation enthalpy of titanium and nickel, which causes the preferential oxidation of titanium rather than nickel during heat treatment at low oxygen atmosphere and temperature of 500 °C [27]. Moreover, heat treatment could be effective in crystallization and increasing the adhesion of sodium titanate hydrogel layer to the metallic substrate [29].

Since the release of harmful and toxic Ni ions from Nitinol into the human body is a serious concern that causes allergy, inflammation and cell death [32], we have tried to minimize that

with pretreatment process. According to findings, the concentration of Ni ions released from the as-received Nitinol with a surface area of about 1 cm^2 into Ringer's solution at 37 °C during 10 days is determined to be about 126.6 ppb, whereas this amount decreases to about 5.3 ppb by pretreatment. The results indicate that pretreatment of Nitinol using a combination of acid-etching, boiling in water and alkaline-heat treatment could provide a good protection ability against Ni ions release. This is mainly owing to decreasing the concentration of Ni ions at the surface and formation of a reliable passive layer during pretreatment. In this case,

releasing the Ni ions accumulated in depth occurs through the surface defects of the pretreated sample. It should be mentioned that according to data from the Agency for Toxic Substances and Disease Registry (ATSDR), the minimal risk level (MRL) of Ni is 0.0002 mg/m^3 (200 ppb). This MRL is based on a no-observed-adverse-effect level (NOAEL) of 0.06 mg Ni/m^3 and a lowest-observed-adverse-effect level (LOAEL) of 0.11 mg Ni/m^3 for chronic inflammation in rats, which were exposed to nickel sulfate for 6 hours/day and 5 days/week during 13 weeks [33]. Hence, the amount of Ni ions release obtained for both as-received and pretreated samples with a surface area of about 1 cm^2 is satisfied. However, the lower releasing of Ni ions from the pretreated sample provides a possibility of using the implants with larger size without any concerning about its safety for the body.

Finally, to investigate the effect of pretreatment on the superelastic behavior of Nitinol, the stress-strain curves of the as-received and pretreated Nitinol samples are illustrated in Fig. 5. It is observed that the as-received sample displays mechanical hysteresis and a linear superelastic behavior with the recoverable strain of about 4.1% after unloading. The absence of the stress plateau in the relevant curve (see Fig. 5a) is related to the fact that the as-received sample is in cold drawn state, which results in the formation of the stress induced martensitic phase. On the contrary, the stress plateau observed in the stress-strain curve of the pretreated sample in Fig. 5b is related to the stress-induced martensitic transformation at the constant stress accompanied with its detwinning during loading and reverse transformation of martensite to austenite in unloading [34]. Moreover, pretreatment not only has no negative effect, but

also slightly improves the superelasticity of Nitinol so that the strain reversibility of about 4.8% is obtained at the human body temperature for the pretreated sample. This could be due to developing Ni_4Ti_3 precipitates during heat treatment, which cause an increasing in the critical stress for plastic deformation by slip mechanism rather than the martensitic transformation [34, 35].

3.2. Characterization of the HA/CS coating

In the following, we used the next layer containing HA particles in a CS matrix to improve the bioactivity and antibacterial properties on the surface of pretreated Nitinol. For applying a uniform and crack free HA/CS coating, three different voltages of 30, 40 and 50 V/cm^2 was employed. The variation of current density with time during EPD of the HA/CS coating at these voltages is illustrated in Fig. 6. According to results, the current density drops at each voltage in the beginning of EPD process mainly owing to deposition of the high resistance HA/CS coating on the sample and then reaches to an almost constant value. The current density in the coated samples could be passed through the pores of the coating. Moreover, the water molecules presence in the wet coating could transmit the current during the EPD process. As expected, the higher voltage provides the higher current densities and the more driving force for the movement of the charged particles toward the cathode.

The weight variation of the HA/CS coating deposited from the suspension containing 0.5g/L CS and 5 g/L HA as a function of time at voltages of 30, 40 and 50 V/cm^2 is also depicted in Fig. 7. As it is seen, the weight of coating applied at all voltages increases with time in an almost linear

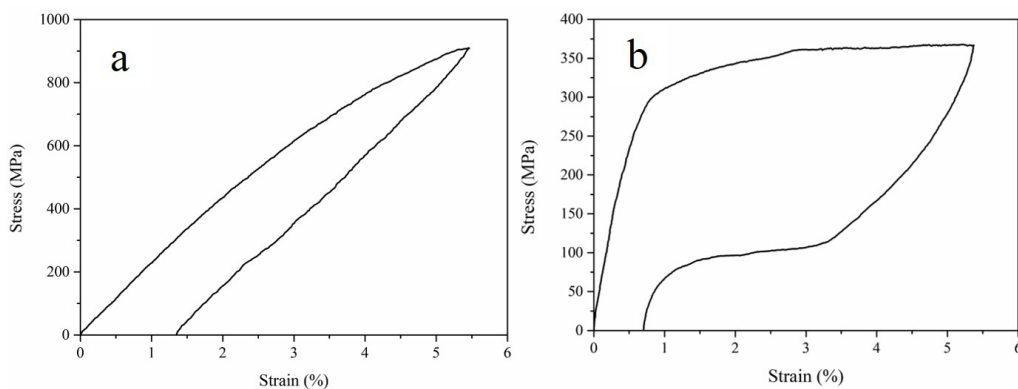


Fig. 5- Stress-strain curves of a) as-received and b) pretreated Nitinol samples at 37°C .

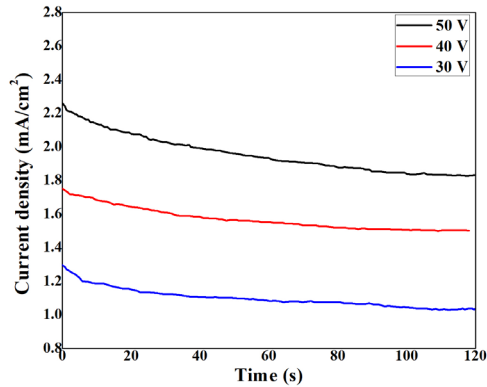


Fig. 6- Current density variations as a function of time during EPD of the HA/CS coating at three different voltages of 30, 40 and 50 V/cm².

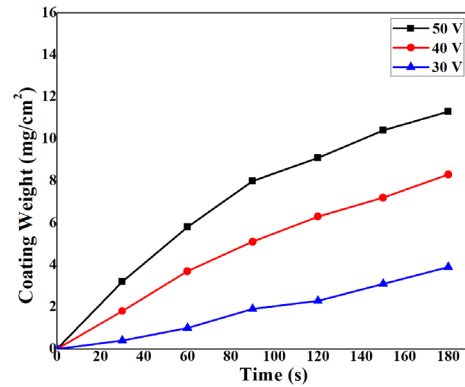


Fig. 7- Changing the weight of HA/CS coating during EPD at three voltages of 30, 40 and 50 V/cm².

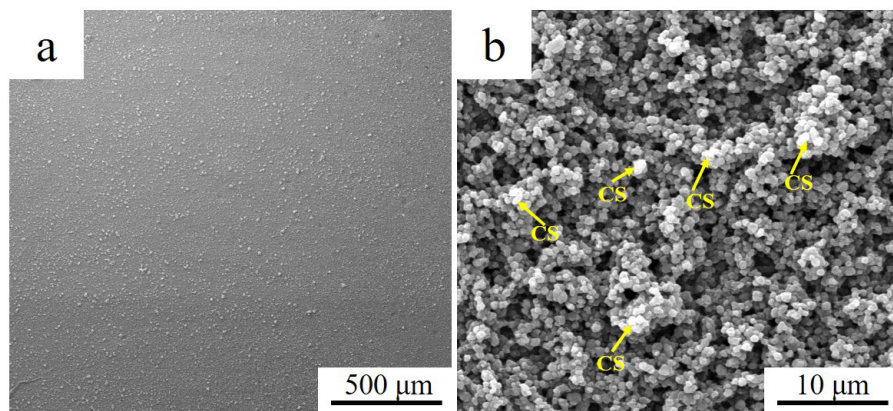


Fig. 8- SEM micrographs of the HA/CS coating applied by EPD from the suspension containing 5 g/L HA and 0.5 g/L CS at 40 V/Cm² for 120 s at a) 100 x and b) 5000 x magnification.

trend according to the Hamaker equation (eq. 1).

$$W=C\mu.A.E.t \quad (\text{eq. 1})$$

Where "W" is the coating weight, "t" is the EPD duration, "E" is the applied electric field, "C" is the particle concentration, " μ " and "A" are the particle mobility and the surface area of the sample, respectively [13, 36].

The slope of the weight-time curve could be also used to evaluate the rate of EPD. It is observable from Fig. 7 that the EPD rate increases at the higher applied voltages. As a matter of fact, EPD is a colloidal process in which the charged particles move under the electric field toward the conductive electrode with opposite charge to deposit on its surface. Therefore, the more electrophoretic mobility of particles under the strong electric field caused by higher applied voltages could effectively

increase the coating weight and so the rate of EPD.

Based on our findings, the visual appearance of the HA/CS coating applied at 30 and 50 V/cm² is unsatisfactory. In contrast, a uniform and crack free coating with acceptable appearance quality could be obtained by EPD at 40 V/cm², which has the ability to fully cover the surface of the pretreated Nitinol. Hence, the samples coated at 40 V/cm² has been used for the further structural and chemical characterization. Fig. 8 shows the SEM image of the HA/CS coating applied at this voltage for 120 s. According to high-magnification SEM micrograph in Fig. 8 b, this coating has the porous microstructure. The pores appeared in this microstructure could be attributed to the hydrogen evolution during EPD at the cathodic surface of the pretreated Nitinol [21].

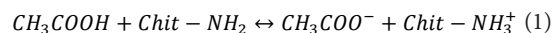
The FTIR analysis is also performed to determine the chemical bands in the HA powder extracted

from bovine cortical bone, medium molecular weight CS purchased from Sigma Aldrich and the CS/HA composite coating applied by EPD method. The corresponding FTIR spectra are depicted in Fig. 9. In the case of HA and HA/CS composite samples (see Figs. 9a and b), the intense infrared bands at 568, 602 and 1031 cm⁻¹ are attributed to the phosphate groups of HA [13, 38]. The characteristic bands of carbonate are appeared at 872 and between 1400-1500 cm⁻¹, demonstrating the partial replacement of phosphate groups (PO_4^{3-}) by carbonates [39]. The adsorption bands present at wavenumbers of 639 and 3572 cm⁻¹ are attributed to hydroxyl stretching mode [23, 38]. The broad adsorption band of water is also appeared between 3350 and 3550 cm⁻¹ [9]. Moreover, the chemical bands related to CS can be seen in the insert in Fig. 9. The basic spectral bands of CS are C-N stretching vibration (1030, 1259 cm⁻¹) [9, 40], C-O stretch of acetyl group (1091 cm⁻¹), C-O-C stretch (1157 cm⁻¹), the amide III band overlapped with C-N stretch (1381 cm⁻¹) [40], C-H bending (1331, 1380, 1423 cm⁻¹), C-H stretch of CH_2 group (2871, 2918 cm⁻¹) [12, 40, 41], NH₂ bending in the amide groups (1605 cm⁻¹) [40], C-O stretch and amide II band (1653 cm⁻¹) [41], and OH groups overlapped with stretching vibration of N-H (3441 cm⁻¹) [12, 41]. Comparing the FTIR spectra of HA and HA/CS samples indicates that most of the characteristic bands of CS are overlapped by those of HA as

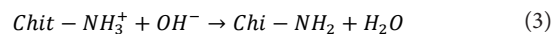
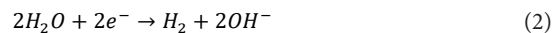
previously reported by Tang et al. [9]. However, the existence of additional bands at around 1647, 2881 and 2927 cm⁻¹ in the FTIR spectrum of the HA/CS coating could be a proof for the adsorption of CS onto the HA particles in this composite coating.

The formation mechanism of the HA/CS composite coating could be described by the co-deposition of HA and CS in the following manner:

CS easily dissolves in the aqueous solution of acetic acid due to the protonation of its amino groups (reaction 1) and behaves as a cationic polyelectrolyte [13, 21, 23]:



When the voltage is applied, the cationic polyelectrolyte CS could accumulate at the cathode surface through their motion under electric field [21]. In the next stage, the water reduction (reaction 2) increases pH at the cathode vicinity and under this conditions the neutralization of the charged macromolecules of CS (reaction 3) results in the deposition of insoluble CS on the surface of the pretreated Nitinol [21, 23].



Moreover, deposition of the coating on the cathodic surface from suspension containing only

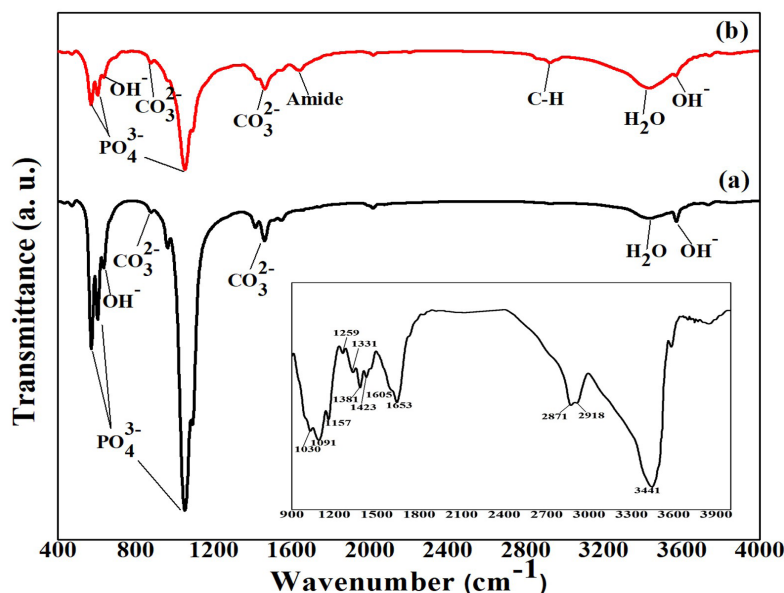


Fig. 9- The FTIR spectra of a) HA powder extracted from bovine cortical bone and b) the composite HA/CS coating applied at 40 V/cm². Insert: FTIR spectrum of CS.

Table 1- The corrosion parameters extrapolated from polarization curves

Samples	I_{corr} ($\mu A/cm^2$)	E_{corr} (mV vs. SCE)
Bare Nitinol	2.63	-301
Pretreated Nitinol	1.94	-160
Pretreated/coated Nitinol	0.75	90

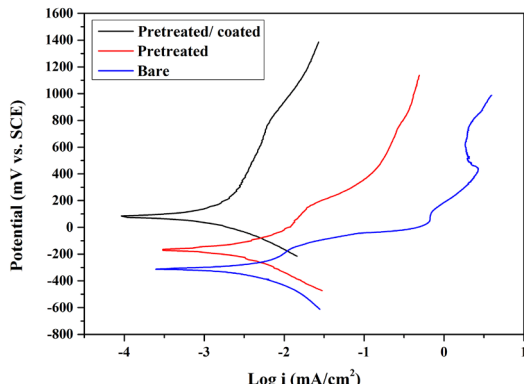


Fig. 10- Potentiodynamic polarization curves of bare, pretreated and coated/pretreated Nitinol alloy in Ringer's solution.

HA particles shows the positive charge of these particles in the mentioned suspension. In fact, HA particles could get the positive charge because of the presence of Ca^+ , $CaOH^+$, and $CaH_2PO_4^+$ on their surface resulted from dissolution and ion exchange between these particles and solution in the pH range of 3–10 [37]. Consequently, both positively charged HA particles and cationic polyelectrolyte CS could be co-deposited on the cathode. In this case, adsorption of CS macromolecules on the surface of HA particles increases the surface charge and the electrostatic stabilization of these particles in the suspension. As a result, the presence of CS improves the EPD process [13, 21]. Moreover, the CS polymer adsorbed on the surface of HA particles could bond these particles together and hold them next to each other in the HA/CS coating (see Fig. 8). Since the concentration of CS in the used suspension is little (0.5 g/l), the volume percentage of the CS polymer surrounding the HA particles is also low in microstructure of this coating.

3.3. Potentiodynamic polarization measurements of the pretreated and coated Nitinol for corrosion behavior

At last, since the implant made of Nitinol alloy should have a good corrosion resistance for preventing Ni ions release and exhibiting the good biocompatibility, the effect of pretreatment and applying the HA/CS composite coating on

the corrosion behavior of this alloy is evaluated by potentiodynamic polarization test. Fig. 10 represents the polarization curves obtained for the bare, pretreated and pretreated-coated Nitinol alloys. Also, the corresponding parameters calculated by Tafel method are listed in Table 1. Compared to bare sample, the corrosion potentials (E_{corr}) of the pretreated and coated samples shift toward more noble potential, indicating the effectiveness of alkaline-heat treatment and applying the HA/CS composite coating on improving the corrosion resistance of Nitinol alloy. Also, it can be seen that the pretreatment decreases the corrosion current and consequently the corrosion rate of Nitinol probably due to the formation of a thin barrier layer consisted of rutile and sodium titanate on its surface. Moreover, applying the HA/CS composite coating on the pretreated Nitinol causes an additional reduction in the corrosion current density, indicating a more protection of this alloy against corrosion. In fact, this coating can act as an excess protective layer and leads to more improvement of corrosion resistance in Ringer's solutions.

4. Conclusion

In this work, the surface modification of Nitinol alloy was studied for enhancing its ability to be used as the metallic implants in the biomedical applications. The surface modification was consisted of the pretreatment of Nitinol and applying the HA/CS composite coating. A combination of chemical etching, boiling in distilled water and alkaline-heat treatment was employed for pretreatment. Also, the HA/CS coating was developed on the pretreated Nitinol by cathodic EPD from suspension containing HA and CS at room temperature. The SEM images showed the porous and warm-like microstructure for the surface layer formed on the pretreated Nitinol. The results of EDS, Raman and GIB analysis proved that this layer was consisted of rutile and sodium titanate phases. According to our findings, pretreatment of Nitinol significantly decreased the concentration of Ni ions released into the Ringer's

solution during 10 days immersion from 126.6 ppb to 5.3. Indeed, the chemical etching and boiling of Nitinol in distilled water could reduce the amount of Ni in the surface and moreover the formation of the surface layer during alkaline-heat treatment could provide an inhibition against the Ni ions release. Additionally, pretreatment not only did not have a negative effect on the superelasticity, but also slightly increased the recoverable strain of Nitinol alloy after unloading from 4.1% to 4.8%. This could be owing to increasing the critical stress for plastic deformation by slip as a result of the formation of Ni_4Ti_3 precipitates during heat treatment at 500 °C. Moreover, we used the HA/CS composite coating on the pretreated Nitinol for improving its biocompatibility. The composite coating applied at constant voltage of 40 V/cm² for 120 s was uniform and crack free with acceptable visual appearance and having the ability of covering the whole surface of the pretreated Nitinol. Moreover, the results of FTIR analysis confirmed the presence of HA and CS in this coating. At last, the results of potentiodynamic polarization studies in the Ringer's solution indicated that the value of i_{corr} for the Nitinol alloy remarkably decreased from 2.63 to 1.94 and 0.75 $\mu\text{A}/\text{cm}^2$, respectively, by pretreatment and applying the HA/CS composite coating. In conclusion, both pretreatment and HA/CS coating could reduce the corrosion rate of Nitinol. It is worthy to note that the protection of Nitinol against corrosion could be effective in decreasing the Ni ions release.

References

- Maleki-Ghaleh H, Khalili V, Khalil-Allafi J, Javidi M. Hydroxyapatite coating on NiTi shape memory alloy by electrophoretic deposition process. *Surface and Coatings Technology*. 2012;208:57-63.
- Qiu D, Wang A, Yin Y. Characterization and corrosion behavior of hydroxyapatite/zirconia composite coating on NiTi fabricated by electrochemical deposition. *Applied Surface Science*. 2010;257(5):1774-8.
- Khalili V, Khalil-Allafi J, Sengstock C, Motemani Y, Paulsen A, Frenzel J, et al. Characterization of mechanical properties of hydroxyapatite-silicon-multi walled carbon nano tubes composite coatings synthesized by EPD on NiTi alloys for biomedical application. *Journal of the Mechanical Behavior of Biomedical Materials*. 2016;59:337-52.
- Constant C, Nichols S, Wagnac É, Petit Y, Desrochers A, Brailovski V. Biocompatibility and mechanical stability of Nitinol as biomaterial for intra-articular prosthetic devices. *Materialia*. 2020;9:100567.
- Chakraborty R, Raza MS, Datta S, Saha P. Synthesis and characterization of nickel free titanium-hydroxyapatite composite coating over Nitinol surface through in-situ laser cladding and alloying. *Surface and Coatings Technology*. 2019;358:539-50.
- Sheykholeslami SOR, Fathyunes L, Etminanfar M, Khalil-Allafi J. In-vitro biological behavior of calcium phosphate coating applied on nanostructure surface of anodized Nitinol alloy. *Materials Research Express*. 2019;6(9):095407.
- Shabalovskaya SA, Anderegg J, Laab F, Thiel PA, Rondelli G. Surface conditions of Nitinol wires, tubing, and as-cast alloys. The effect of chemical etching, aging in boiling water, and heat treatment. *Journal of Biomedical Materials Research*. 2003;65B(1):193-203.
- Etminanfar MR, Khalil-Allafi J, Montaseri A, Vatankhah-Barenji R. Endothelialization and the bioactivity of Ca-P coatings of different Ca/P stoichiometry electrodeposited on the Nitinol superelastic alloy. *Materials Science and Engineering: C*. 2016;62:28-35.
- Tang S, Tian B, Guo Y-J, Zhu Z-A, Guo Y-P. Chitosan/carbonated hydroxyapatite composite coatings: Fabrication, structure and biocompatibility. *Surface and Coatings Technology*. 2014;251:210-6.
- Say Y, Aksakal B. Enhanced corrosion properties of biological NiTi alloy by hydroxyapatite and bioglass based biocomposite coatings. *Journal of Materials Research and Technology*. 2020;9(2):1742-9.
- Fathyunes L, Khalil-Allafi J, Moosavifar M. Development of graphene oxide/calcium phosphate coating by pulse electrodeposition on anodized titanium: Biocorrosion and mechanical behavior. *Journal of the Mechanical Behavior of Biomedical Materials*. 2019;90:575-86.
- Zhong Z, Qin J, Ma J. Cellulose acetate/hydroxyapatite-chitosan coatings for improved corrosion resistance and bioactivity. *Materials Science and Engineering: C*. 2015;49:251-5.
- Mahmoodi S, Sorkhi L, Farrokhi-Rad M, Shahrami T. Electrophoretic deposition of hydroxyapatite-chitosan nanocomposite coatings in different alcohols. *Surface and Coatings Technology*. 2013;216:106-14.
- Su Y, Cockerill I, Zheng Y, Tang L, Qin Y-X, Zhu D. Biofunctionalization of metallic implants by calcium phosphate coatings. *Bioact Mater*. 2019;4:196-206.
- Pang X, Zhitomirsky I. Electrodeposition of hydroxyapatite-silver-chitosan nanocomposite coatings. *Surface and Coatings Technology*. 2008;202(16):3815-21.
- Avcu E, Baştan FE, Abdullah HZ, Rehman MAU, Avcu YY, Boccaccini AR. Electrophoretic deposition of chitosan-based composite coatings for biomedical applications: A review. *Progress in Materials Science*. 2019;103:69-108.
- Frank LA, Onzi GR, Morawski AS, Pohlmann AR, Gutierrez SS, Contri RV. Chitosan as a coating material for nanoparticles intended for biomedical applications. *Reactive and Functional Polymers*. 2020;147:104459.
- Karimi N, Kharazia M, Raeissi K. Electrophoretic deposition of chitosan reinforced graphene oxide-hydroxyapatite on the anodized titanium to improve biological and electrochemical characteristics. *Materials Science and Engineering: C*. 2019;98:140-52.
- Hahn B-D, Park D-S, Choi J-J, Ryu J, Yoon W-H, Choi J-H, et al. Aerosol deposition of hydroxyapatite-chitosan composite coatings on biodegradable magnesium alloy. *Surface and Coatings Technology*. 2011;205(8-9):3112-8.
- Grandfield K, Zhitomirsky I. Electrophoretic deposition of composite hydroxyapatite-silica-chitosan coatings. *Materials Characterization*. 2008;59(1):61-7.
- Pang X, Zhitomirsky I. Electrophoretic deposition of composite hydroxyapatite-chitosan coatings. *Materials Characterization*. 2007;58(4):339-48.
- Song L, Gan L, Xiao Y-F, Wu Y, Wu F, Gu Z-W. Antibacterial

- hydroxyapatite/chitosan complex coatings with superior osteoblastic cell response. *Materials Letters*. 2011;65(6):974-7.
23. Yan Y, Zhang X, Li C, Huang Y, Ding Q, Pang X. Preparation and characterization of chitosan-silver/hydroxyapatite composite coatings on TiO₂ nanotube for biomedical applications. *Applied Surface Science*. 2015;332:62-9.
24. Kim H-M, Miyaji F, Kokubo T, Nakamura T. Preparation of bioactive Ti and its alloys via simple chemical surface treatment. *Journal of Biomedical Materials Research*. 1996;32(3):409-17.
25. Liu X, Chu P, Ding C. Surface modification of titanium, titanium alloys, and related materials for biomedical applications. *Materials Science and Engineering: R: Reports*. 2004;47(3-4):49-121.
26. Fatehi K, Moztarzadeh F, Solati-Hashjin M, Tahriri M, Rezvannia M, Saboori A. Biomimetic hydroxyapatite coatings deposited onto heat and alkali treated Ti6Al4V surface. *Surface Engineering*. 2009;25(8):583-8.
27. Shabalovskaya S, Anderegg J, Van Humbeeck J. Critical overview of Nitinol surfaces and their modifications for medical applications. *Acta Biomaterialia*. 2008;4(3):447-67.
28. Bionanomaterials for Dental Applications: Jenny Stanford Publishing; 2012 2012/10/26.
29. Escada ALA, Machado JPB, Schneider SG, Rezende MCRA, Claro APRA. Biomimetic calcium phosphate coating on Ti-7.5Mo alloy for dental application. *Journal of Materials Science: Materials in Medicine*. 2011;22(11):2457-65.
30. Meng F, Liu Y, Xue T, Su Q, Wang W, Qi T. Structures, formation mechanisms, and ion-exchange properties of α -, β -, and γ -Na₂TiO₃. *RSC Advances*. 2016;6(113):112625-33.
31. Bamberger CE, Begun GM. Sodium Titanates: Stoichiometry and Raman Spectra. *Journal of the American Ceramic Society*. 1987;70(3):C-48-C-51.
32. Sevcikova J, Pavkova Goldbergova M. Biocompatibility of NiTi alloys in the cell behaviour. *BioMetals*. 2017;30(2):163-9.
33. Toxicological Profile for Polycyclic Aromatic Hydrocarbons, U.S. Department of Health & Human Services, Public Health Service, Agency for Toxic Substances and Disease Registry, Washington, D.C., August, 1985. *Journal of Toxicology: Cutaneous and Ocular Toxicology*. 1999;18(2):141-7.
34. Kazemi-Choobi K, Khalil-Allafi J, Abbas-Chianeh V. Influence of recrystallization and subsequent aging treatment on superelastic behavior and martensitic transformation of Ni50.9Ti wires. *Journal of Alloys and Compounds*. 2014;582:348-54.
35. Wang X, Kustov S, Li K, Schryvers D, Verlinden B, Van Humbeeck J. Effect of nanoprecipitates on the transformation behavior and functional properties of a Ti-50.8 at.% Ni alloy with micron-sized grains. *Acta Materialia*. 2015;82:224-33.
36. Hamaker HC. Formation of a deposit by electrophoresis. *Transactions of the Faraday Society*. 1940;35:279.
37. Pang X, Zhitomirsky I. Electrodeposition of composite hydroxyapatite-chitosan films. *Materials Chemistry and Physics*. 2005;94(2-3):245-51.
38. Fathyunes L, Khalil-Allafi J, Moosavifar M. Development of graphene oxide/calcium phosphate coating by pulse electrodeposition on anodized titanium: Biocorrosion and mechanical behavior. *Journal of the mechanical behavior of biomedical materials*. 2019 Feb 1;90:575-86.
39. Fathyunes L, Khalil-Allafi J. Effect of employing ultrasonic waves during pulse electrochemical deposition on the characteristics and biocompatibility of calcium phosphate coatings. *Ultrasonics Sonochemistry*. 2018;42:293-302.
40. Kumari S, Rath P, Sri Hari Kumar A, Tiwari TN. Extraction and characterization of chitin and chitosan from fishery waste by chemical method. *Environmental Technology & Innovation*. 2015;3:77-85.
41. Archana D, Singh BK, Dutta J, Dutta PK. In vivo evaluation of chitosan-PVP-titanium dioxide nanocomposite as wound dressing material. *Carbohydrate Polymers*. 2013;95(1):530-9.